

Influence of temperature and internal electric field on light emission in wurtzite GaN/AlGa_xN nanowire heterostructures

M. ZHANG^{a,*}, J. J. SHI^b

^aCollege of Physics and Electron Information, Inner Mongolia Normal University, Hohhot 010022, People's Republic of China

^bState Key Laboratory for Mesoscopic Physics, and Department of Physics, Peking University, Beijing 100871, People's Republic of China

Within the framework of the effective-mass approximation, the influence of the temperature and the internal electric field on the confined exciton energy shift in [0001]-oriented GaN/AlGa_xN strained wurtzite nanowire heterostructures is investigated by using the variational approach, in which the important dielectric mismatch is considered. Our results show that the temperature, the strong built-in electric field and the quantum dot (QD) geometrical parameter have a significant influence on the luminescent characteristics of the exciton states. The emission wavelength has a red-shift if the temperature (QD height or the nanowire diameter) increases. Our calculations also indicate that the exciton oscillator strength decreases quickly with increasing of the QD height and temperature.

(Received June 24, 2016; accepted February 10, 2017)

Keywords: GaN/AlGa_xN strained nanowire heterostructure, Temperature, Exciton, Optical property

1. Introduction

GaN is an important wide direct band gap semiconductor material, which has various applications in blue and ultraviolet light emission, high-temperature and high-power electronic devices. With the development of the chemical vapor deposition method and molecular-beam epitaxy, high-quality GaN nanowires (NWs) were successfully synthesized with exceptional optical and transport properties [1–3]. GaN NWs are widely considered as nanostructures exhibiting an extremely low density of structural defects and extend the involved optical transitions to the ultraviolet region due to their quantum confinement effect. Hence GaN NWs have attracted much attention in recent years.

It has been known that the quantum dots (QDs) embedded in a nanowire exhibit strong photon antibunching, typically an order of magnitude brighter than self-assembled QDs [4]. In axial AlGa_xN/GaN wurtzite nanowire heterostructures (NWHs), due to the lattice mismatch along the growth axis between Al_xGa_{1-x}N and GaN layers, a strong built-in electric field (BEF) can be induced by the piezoelectric and spontaneous polarizations [5]. It is the primary reason for the large red-shift of the photoluminescence (PL) emission peaks. Thus, III-nitride NWs and NWHs are considered as a promising material for the improved optoelectronic nano-devices.

Recently, the photoluminescence (PL) and Raman spectra of GaN/AlGa_xN NWHs have been investigated.

Furtmayr and co-workers performed a careful study of the three-dimensional carrier confinement in GaN/Al_xGa_{1-x}N ($0 < x \leq 1$) NWHs and analyzed their PL characteristics for different Al concentrations from $x = 0.08$ to 1 [6]. The electronic structure and optical properties of GaN/AlGa_xN core/shell NWs with hexagonal and triangular cross sections are studied theoretically [7]. A microphotoluminescence of single GaN/AlN QD embedded in single NW has been investigated [8]. The single exciton line with full width at half-maximum as narrow as 1 meV is observed at low excitation power. The PL investigations of GaN/Al_xGa_{1-x}N QDs embedded in NWs show that the BEF is significantly smaller than the value expected from the spontaneous polarization discontinuity [9]. The growth and structural properties of GaN/AlN core-shell NWHs have been studied using a combination of resonant x -ray diffraction, Raman spectroscopy and high resolution transmission electron microscopy experiments [10].

The excitons and related issues have also been studied in vertically coupled quantum dots (VCQDs), in which the nonparabolic Stark effect has been found [11]. Exciton binding energy, interband emission energy and some non-linear optical properties in QDs are investigated in the presence of pressure and temperature [12]. So far, the relation between structural characteristics and optical properties has been well understood in two-dimensional AlGa_xN/GaN heterostructures. It is imperative to investigate the optical and transport properties of exciton confined in GaN/Al_xGa_{1-x}N NWHs for achieving the

optimum performance of GaN NW-based optoelectronic nano-devices.

To the best of our knowledge, the theoretical investigation about the influence of temperature and the BEF on the optical properties of confined exciton states in strained wurtzite GaN/AlGaIn NWs is still absent up to now. We thus pay our attention to the influence of temperature and BEF on the exciton energy shift in GaN/Al_xGa_{1-x}N wurtzite NWs. This will allow us to highlight the effect of the temperature and BEF on the light emission of exciton.

2. Model and theory

To investigate the influence of the BEF and temperature on the shift of the binding energy of the electron-heavy-hole exciton confined in GaN/Al_xGa_{1-x}N NWs with radius R , we can write the exciton effective-mass Hamiltonian in cylindrical coordinates as follows,

$$\hat{H} = -\sum_{i=e,h} \frac{\hbar^2}{2} \left\{ \frac{1}{m_{\perp i}} \left[\frac{1}{\rho_i} \frac{\partial}{\partial \rho_i} \left(\rho_i \frac{\partial}{\partial \rho_i} \right) + \frac{1}{\rho_i^2} \frac{\partial^2}{\partial \theta_i^2} \right] \right\} + \sum_{i=e,h} \left[-\frac{\hbar^2}{2} \frac{1}{m_{z i}} \frac{\partial^2}{\partial z_i^2} + V(\rho_i, z_i) \mp eFz_i \right] - \frac{e^2}{4\pi\bar{\epsilon}\epsilon_0 |\vec{r}_e - \vec{r}_h|} \quad (1)$$

where the subscript $i=e$ or h denotes the electron or heavy hole, $m_{z i}$ and $m_{\perp i}$ are the effective mass of the electron (heavy-hole) along and perpendicular to the [0001]-oriented (z -direction) GaN/Al_xGa_{1-x}N wurtzite NWs.

In wurtzite phase, GaN and AlN have a direct gap and an indirect gap at the Γ -symmetry point, respectively. The compound alloy Al_xGa_{1-x}N thus presents a direct to an indirect Γ -X gap transition when $x > 0.53$ (Ref. [13]). The bowing dependence of the Al_xGa_{1-x}N gap energy on x is given by,

$$E_{g, \text{Al}_x\text{Ga}_{1-x}\text{N}}(x) = (1-x)E_{g, \text{GaN}} + xE_{g, \text{AlN}} + bx(x-1), \quad (2)$$

where $b = 1.0$ eV is the bowing parameter [14]. The temperature dependent band gap in different materials at Γ -point can be given by the empirical Varshni equation [15],

$$E_g = E_g(0) - \frac{\alpha T^2}{\beta + T}, \quad (3)$$

where $E_g(0)$ is the energy gap at 0K, α and β are adjustable Varshni parameters.

In Eq. (1), F is the BEF due to the piezoelectricity and spontaneous polarization in the GaN/Al_xGa_{1-x}N NWs and can be given by,

$$F = \frac{P_{\text{GaN}}^{\text{SP}} + P_{\text{GaN}}^{\text{PE}} - P_{\text{AlGaIn}}^{\text{SP}}}{\epsilon_{\text{GaN}}\epsilon_0}, \quad (4)$$

where P^{SP} (P^{PE}) denotes the spontaneous (piezoelectric) polarization intensity. The strain induced piezoelectric field in [0001]-oriented wurtzite structures is given by [16]

$$P_{[0001]}^{\text{PE}} = 2d_{31}(C_{11} + C_{12} - \frac{2C_{13}^2}{C_{33}})\epsilon_{xx}, \quad (5)$$

In Eq. (1), $\bar{\epsilon}$ is a mean value of the dielectric constant between the electron and hole. Considering the dielectric-constant mismatch between AlGaIn and GaN materials, two important effects must be included. One depends on the amount of the exciton wave function in GaN layer, and the other on the strength and position of the image charges. For simplicity, the complicated dielectric mismatch between the NW and vacuum is ignored here due to an infinity potential barrier in vacuum. Following Ref. [17], we can define $\bar{\epsilon}$ as follows,

$$\bar{\epsilon} = \sqrt{\beta_e \beta_h} \epsilon_{\text{GaN}} + (1 - \sqrt{\beta_e \beta_h}) \epsilon_{\text{AlGaIn}}, \quad (6)$$

where β_e and β_h are the weighting parameters and can be defined as $\beta_i = H_D(2/\kappa_{i, \text{AlGaIn}} + H_D)(i=e, h)$, where $\kappa_{i, \text{AlGaIn}}$ is the characteristic wave vectors of the electron or hole in AlGaIn.

We choose the electron or hole wave function with the following general form

$$\psi_i(\rho_i, \theta_i, z_i) = J_m(\rho_i) \xi(z_i) e^{im\theta_i}, \quad m = 0, \pm 1, \pm 2, \dots, \quad (7)$$

Considering the correlation of the electron-hole relative motion, the trial wave function of the exciton confined in GaN/Al_xGa_{1-x}N NWs can be written as,

$$\Phi(\vec{r}_e, \vec{r}_h) = \psi_e(\rho_e, \theta_e, z_e) \psi_h(\rho_h, \theta_h, z_h) e^{-\alpha \rho_{\text{eh}}^2} e^{-\beta z_{\text{eh}}^2}, \quad (8)$$

where $\rho_{\text{eh}}^2 = (x_e - x_h)^2 + (y_e - y_h)^2$ and $z_{\text{eh}} = z_e - z_h$, the variational parameter α is responsible for the in-plane correlation, and β accounts for the correlation of the relative motion in the z -direction.

The binding energy of the excitonic system is defined as

$$E_b = E_g + E_e + E_h - E_{ex}, \quad (9)$$

where E_e (E_h) is the electron (hole) confinement energy and E_g is the band gap of GaN QDs, and E_{ex} is the exciton energy.

We adopt the formulae of Ref. [17] to approximately estimate the increment of the exciton binding energy due to the image charges,

$$\Delta E_b = 2 \frac{\epsilon_{\text{GaN}} - \epsilon_{\text{AlGaIn}}}{\epsilon_{\text{GaN}} + \epsilon_{\text{AlGaIn}}} \frac{e^2}{\epsilon_{\text{GaN}} a_0} \frac{I(H_D/a_0)}{H_D/a_0}, \quad (10)$$

where a_0 is the exciton Bohr radius, and the function $I(t)$ is defined as,

$$I(t) = \int_0^\infty \frac{(2t)^3}{[x^2 + (2t)^2]^{3/2}} \frac{e^{-x}}{[1 + (x/2\pi)^2]^2} \left[\frac{\sinh(x/2)}{x/2} \right]^2 dx. \quad (11)$$

The exciton oscillator strength is imperative especially in the study of optical properties and is related to the electronic dipole allowed absorption. The oscillator strength for the exciton ground state is given by [18],

$$f_{ex} = \frac{2P^2}{m_0(E_{ex} - E_0)} \left| \int \Phi(\vec{r}_e, \vec{r}_h) d\vec{r}_e \right|^2, \quad (12)$$

where P describes all intracell matrix-element effects, m_0 is the bare electron mass, and E_0 is the energy of the state without the exciton effect.

Table 1. Lattice constant a and c , band gap E_g , temperature coefficients α and β , and effective masses m_e and m_h for GaN and AlN

Material	$a(\text{\AA})$	$c(\text{\AA})$	$E_g(\text{eV})$	α (meV/K)	β (meV/K)	$m_{\perp e}$	m_{ze}	$m_{\perp h}$	m_{zh}
GaN	3.189 ^[19]	5.185 ^[19]	3.507 ^[19]	0.909 ^[19]	1.799 ^[19]	0.20 ^[19]	0.20 ^[19]	1.76 ^[20]	1.61 ^[20]
AlN	3.112 ^[19]	4.982 ^[19]	6.23 ^[19]	830 ^[19]	1462 ^[19]	0.28 ^[19]	0.32 ^[19]	1.949 ^[20]	2.584 ^[20]

Table 2. The elastic constant C_{11} , C_{12} , C_{13} and C_{33} , the relevant piezoelectric constant d_{31} , static dielectric constant ϵ and spontaneous polarization P^{sp} for GaN and AlN

Material	$C_{11}(\text{GPa})$	$C_{12}(\text{GPa})$	$C_{13}(\text{GPa})$	$C_{33}(\text{GPa})$	d_{31} (10^{-10} cm/V)	ϵ	P^{sp} (C/m ²)
GaN	365 ^[21]	139 ^[21]	101 ^[21]	405 ^[21]	-1.7 ^[22]	9.28 ^[23]	-0.029 ^[24]
AlN	397 ^[21]	143 ^[21]	112 ^[21]	371 ^[21]	-2.0 ^[22]	8.67 ^[23]	-0.081 ^[24]

Fig. 1(a) depicts the variation of the exciton binding energy as a function of the QD height in the presence of temperature and with the nanowire radius $R = 5$ nm. We can find that the binding energy increases with decreasing of H_D . In order to clarify the influence of the strong BEF and dielectric-constant mismatch, the corresponding results without the BEF and dielectric-constant mismatch are also proposed. It clearly indicates that the BEF dramatically reduces the exciton binding energy. The Coulomb interaction between the electron and hole is reduced in virtue of increase in their relative distance in the z -direction. This ultimately causes the decrease of the exciton binding energy when the dot height increases or the BEF is considered. Moreover, we note that the exciton binding energy decreases if temperature increases for a given NWHs. This is because the red-shift of the effective band gap of the GaN QD due to the strong BEF and

3. Numerical results and discussion

Considering the influence of the BEF, temperature and dielectric-constant mismatch effect, we calculate the exciton binding energy and analyze the optical properties in a strained cylindrical nanowire heterojunction. All of the material parameters used in our calculations are summarized in Tables 1 and 2. The ratio of the conduction band to the valence band offset is given to be 65:20 [25]. The parameters of the $\text{Al}_x\text{Ga}_{1-x}\text{N}$ ternary alloy can be derived from a linear combination between the binary constituents AlN and GaN.

temperature T . Moreover, the results also show that the temperature plays an important role in the exciton binding energy if the BEF effect is considered. For example, the binding energy increases 5.52 meV (9.7%) for the NWH with $H_D=2$ nm when T increases from 0 to 300 K, in which the BEF and dielectric mismatch effects are included. The corresponding difference is of 1.89 meV (2.7%) for the case of the zero electric field. The results also show the effect of BEF on the exciton binding energy is distinctly stronger than the effect of temperature. Furthermore, we have also completed our calculations without the dielectric-constant mismatch effects (see the dash-dot line). It can be seen that the dielectric-constant mismatch has a definite influence on the exciton binding energy. Generally, E_b increases if the dielectric-constant mismatch is considered. For instance, if $H_D=2\text{nm}$ and $T=0\text{K}$, the

exciton binding energy increases 1.45 meV (3.79%), which shows a small energy shift.

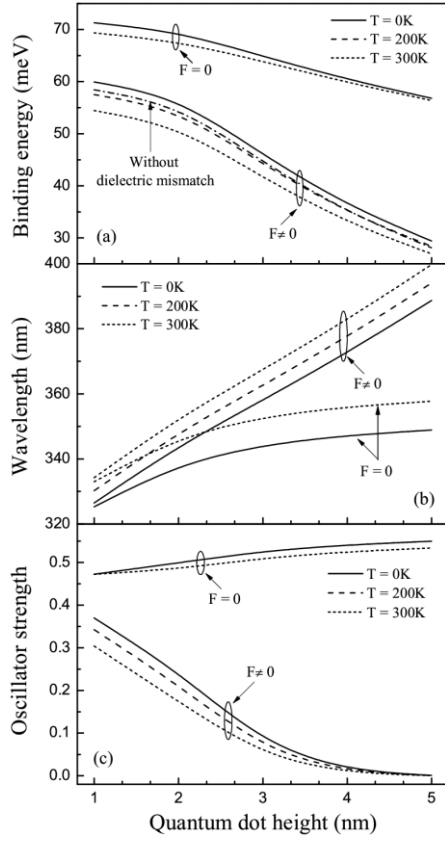


Fig. 1. The heavy-hole exciton binding energy (a), the emission wavelength (b) and the exciton oscillator strength (c) as a function of the quantum dot height in cylindrical wurtzite Al_{0.2}Ga_{0.8}N/GaN strained NWHs with different temperatures

We can see from Fig. 1(b) that the emission wavelength λ monotonically increases if QD height increases. By comparing the results with or without the BEF, we find that the change of the wavelength λ becomes more sensitive to the QD height if considering the BEF. It also reveals that the emission wavelength shifts to the long wave side, namely, red shift. Furthermore, Fig. 1(b) shows that the emission wavelength increases when the temperature T increases. For the QD height $H_D=2$ nm, the emission wavelength is $\lambda=344$ (352.6) nm if $T = 0$ (300) K. The difference (relative difference) is $\Delta\lambda = 8.6$ nm (2.5%). Hence, the temperature, BEF and strong exciton confinement have an obvious influence on the electronic structures and optical properties of Al_{0.2}Ga_{0.8}N/GaN strained NWHs.

The temperature dependence of the oscillator strength as a function of the QD height in the Al_{0.2}Ga_{0.8}N/GaN strained NWHs is shown in Fig. 1(c). It is observed that the f_{ex} decreases markedly because the electron-hole

spatial separation in the z -direction becomes large with increasing of H_D . When $H_D \geq 4.5$ nm, the overlap integral between the electron and hole wave functions approaches zero, so $f_{ex} \approx 0$. Moreover, we note that the increase of temperature causes the oscillator strength to decline further. Especially for small height QD, this trend is more significant. For example, when T increases from 0 to 300K, the variation of f_{ex} at $H_D = 2$ nm is 0.07 with a percentage of 28.7%.

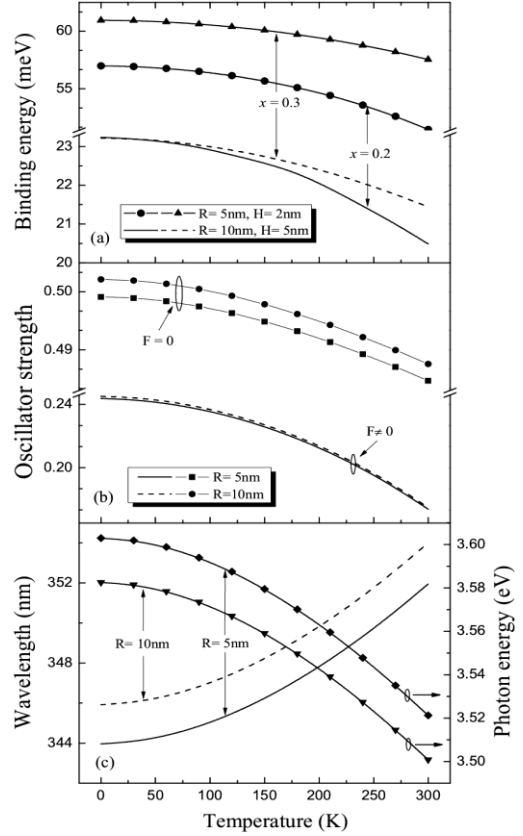


Fig. 2. The heavy-hole exciton binding energy (a), the oscillator strength (b), the emission wavelength and the photon energy (c) as a function of the temperature T with different nanowire radius and Al component

The exciton binding energy, exciton oscillator strength, emission wavelength and photon energy as a function of the temperature T in wurtzite GaN/Al_xGa_{1-x}N strained NWHs with different nanowire radius and Al component are illustrated in Fig. 2. We can find from Fig. 2(a) that the exciton binding energy decreases monotonically as T increases, which is consistent with Fig. 1(a). As T increases, the binding energy changes slowly, but we note that an obvious decreasing tendency for $T \geq 100$ K. The temperature effects become more obvious for the small height (radius) QDs than the large height (radius) QDs. Moreover, it is observed that the increase of Al component x enhances the exciton binding energy obviously. This is because the Al component can adjust

the barrier height effectively which leads to the enhancement of the exciton localization, so the binding energy shifts toward the higher energy. For instance, if $R = 5$ nm, $H_D = 2$ nm and $T = 200$ K, the net increment of the exciton binding energy for the two cases of $x = 0.2$ and 0.3 is of 4.86 nm with a percentage of 8.93% . The data clearly indicate that the exciton states sensitively depend on the confinement potential.

In Fig. 2(b), we show the exciton oscillator strength f_{ex} as a function of the temperature T in the presence of the polarization field and the dielectric mismatch. For the sake of comparison, the situation of zero field is also presented. We can see from Fig. 2(b) that f_{ex} reduces quickly if temperature increases with or without the BEF. But it can be clearly seen that the temperature dependence is more significant in the presence of BEF. For example, the difference of the oscillator strength f_{ex} between 0 and 300 K is of 28.7% ($F \neq 0$) and 2.89% ($F = 0$) for $R = 5$ nm and $x = 0.2$. Our calculations also show that the oscillator strength f_{ex} increases when R increases and it is almost not changed when the QD radius $R = 10$ nm.

In Fig. 2(c), we plot the influence of temperature on the emission wavelength and photon energy as a function of the QD radius with the height 2 nm. In the figure, the lines (symbols) represent the relationship of emission wavelength (photon energy) and temperature. We can see from Fig. 2(c) that the emission wavelength shows a distinct red shift, whereas the exciton peak energy exhibits a blue shift. The qualitative analysis of Fig. 2(c) are in agreement with the experimental measurements [26]. Fig. 2(c) demonstrates that the interband optical transition energy is affected deeply by the temperature and can not be ignored in the design of optical devices. Fig. 2(c) also indicates that the optical transition energy decreases with increasing of QD radius R . Our calculation results reveal an obvious reduction tendency when the QD radius $R > 5$ nm, then it becomes gentle gradually.

4. Conclusions

Considering the influence of the temperature, the QD height and radius, the strong BEF, and the dielectric mismatch on the exciton binding energy, the emission wavelength and the oscillator strength, we variationally calculate the exciton states confined in a cylindrical wurtzite GaN/Al_xGa_{1-x}N strained NWHs based on the effective mass approximation. We find that the ground state exciton binding energy has a red shift due to the temperature effect in GaN/Al_xGa_{1-x}N strained NWHs. At the same time, the confinement effect on the electron and hole and the strong internal electric field caused by the piezoelectricity and spontaneous polarization decrease the exciton binding energy effectively. With increasing of the QD height or the temperature, the emission wavelength moves toward the long wave direction. Compared with the $F = 0$ case, the emission wavelength also increases due to the BEF effects. However, the oscillator strength decreases

with the increasing of the temperature, and this effect becomes more obviously for the small QD height. The emission photon peak energy shows a blue shift character with increasing of the temperature T , which directly leads to the red shift of the emission wavelength. The dielectric mismatch has a minor effect. All our calculations indicate that the temperature, BEF and the QD geometrical confinement have a remarkable influence on the optical characteristics of the exciton states. The results allow us to achieve a better understanding of the confined exciton emission properties in actual GaN/Al_xGa_{1-x}N strained NWHs, which is very important to GaN-based optoelectronic nano-device applications.

Acknowledgments

This work was supported jointly by the National Natural Science Foundation of China (11364030, 11474012) and the Natural Science Foundation of Inner Mongolia Autonomous Region of China (2015MS0127).

References

- [1] E. Calleja, M. A. Sánchez-García, F. J. Sanchez, F. Calle, F. B. Naranjo, E. Muñoz, U. Jahn, K. Ploog, *Phys. Rev. B* **62**, 6826 (2000).
- [2] E. Calleja, J. Ristić, S. Fernández-Garrido, L. Cerutti, M. A. Sánchez-García, J. Grandal, A. Trampert, U. Jahn, G. Sánchez, A. Griol, B. Sánchez, *Phys. Status Solidi (b)* **244**, 2816 (2007).
- [3] B. Ha, S. H. Seo, J. H. Cho, C. S. Yoon, J. Yoo, G. Yi, C. Y. Park, C. Lee, *J. Phys. Chem. B* **109**, 11095 (2005).
- [4] M. T. Borgström, V. Zwiller, E. Müller, A. Imamoglu, *Nano Lett.* **5**, 1439 (2005).
- [5] J.-M. Wagner, F. Bechstedt, *Phys. Rev. B* **66**, 115202 (2002).
- [6] F. Furtmayr, J. Teubert, P. Beckera, S. Conesa-Bojc, J. R. Morante, J. Arbiol, A. Chernikov, S. Schäfer, S. Chatterjee, M. Eickhoff, *Phys. Rev. B* **84**(20), 205303 (2011).
- [7] B. M. Wong, F. Léonard, Q. Li, G. T. Wang, *Nano Lett.* **11**(8), 3074 (2011).
- [8] J. Renard, R. Songmuang, C. Bougerol, B. Daudin, B. Gayral, *Nano. Lett.* **8**(7), 2092 (2008).
- [9] R. Songmuang, D. Kalita, P. Sinha, M. Den Hertog, R. André, T. Ben, E. Monroy, *Appl. Phys. Lett.* **99**(14), 141914 (2011).
- [10] K. Hestroffer, R. Mata, D. Camacho, *Nanotechnology* **21**(41), 415702 (2011).
- [11] T. Chwiej, S. Bednarek, J. Adamowski, B. Szafran, F. M. Peeters, *J. Lumin.* **112**, 122(2005).
- [12] M. Narayanan, A. John Peter, *Quantum Matter.* **1**, 53 (2012).
- [13] W. J. Fan, M. F. Li, T. C. Chong, J. B. Xia, *J. Appl. Phys.* **79**, 188 (1996).

- [14] F. Yun, M. A. Reshchikov, L. He, T. King, H. Morkoç, C. S. W. Novak, L. Wei, *J. Appl. Phys.* **92**, 4837 (2002).
- [15] Y. P. Varshni, *Physica* **34**, 149 (1967).
- [16] D. L. Smith, C. Mailhot, *Rev. Mod. Phys.* **62**, 173 (1990).
- [17] H. Mathieu, P. Lefebvre, P. Christol, *Phys. Rev. B* **46**, 4092 (1992).
- [18] W. M. Que, *Phys. Rev. B* **45**, 11036 (1992).
- [19] I. Vurgaftman, J. R. Meyer, L. R. Ram-Mohan, *J. Appl. Phys.* **89**, 5815 (2001).
- [20] D. Fritsch, H. Schmidt, M. Grundmann, *Phys. Rev. B* **67**, 235205 (2003).
- [21] S. P. Łepkowski, *Phys. Rev. B* **75**, 195303 (2007).
- [22] G. Martin, A. Botchkarev, A. Rockett, H. Morkoç, *Appl. Phys. Lett.* **68**(18), 2541 (1996).
- [23] V. A. Fonoberov, A. A. Balandin, *J. Appl. Phys.* **94**(11), 7178 (2003).
- [24] V. A. Fonoberov, A. A. Balandin, *J. Vac. Sci. Technol. B* **22**(4), 2190 (2004).
- [25] M. B. Nardelli, K. Rapcewicz, J. Bernholc, *Phys. Rev. B* **55**, R7323 (1997).
- [26] T. Kotani, M. Arita, K. Hoshino, Y. Arakawa, *Appl. Phys. Lett.* **108**, 052102 (2016).

*Corresponding author: smile_zm@126.com